Catal Lett (2008) 122:9–19
DOI 10.1007/s10562-007-9352-x

Low Temperature Water–Gas Shift/Methanol Steam Reforming: Alkali Doping to Facilitate the Scission of Formate and Methoxy C–H Bonds over Pt/ceria Catalyst

Harold N. Evin · Gary Jacobs · Javier Ruiz-Martinez · Uschi M. Graham · Alan Dozier · Gerald Thomas · Burtron H. Davis

Received: 21 September 2007 / Accepted: 7 November 2007 / Published online: 27 November 2007

Abstract Doping Pt/ceria catalysts with the Group 1 alkali metals was found to lead to an important weakening of the C–H bond of formate and methoxy species. This was demonstrated by a shift to lower wavenumbers of the formate and methoxy *v*(CH) vibrational modes by DRIFTS spectroscopy. Li and Na-doped Pt/ceria catalysts were tested relative to the undoped catalyst for low temperature water–gas shift and methanol steam reforming using a fixed bed reactor and exhibited higher catalytic activity. Steaming of formate and methoxy species pre-adsorbed on the catalyst surface during in-situ DRIFTS spectroscopy suggested that the species were more reactive for dehydrogenation steps in the catalytic cycle for the Li and Na-doped catalysts relative to undoped Pt/ceria. However, with increasing atomic number over the series of alkali-doped catalysts, the stability of a fraction of the carbonate species was found to increase. This was observed during TPD-MS measurements of the adsorbed CO_2 probe molecule by a systematic increase of a high temperature peak for a fraction of the CO_2 desorbed. This result indicates that alkali-doping is an optimization problem—that is, while improving the dehydrogenation rates of methoxy and formate species, the carbonate intermediate stability increases, making it difficult to liberate the CO_2. Infrared spectroscopy results of CO adsorbed on Pt and ceria suggest that the alkali dopant is located on, and electronically modifies, both the Pt and ceria components. The results not only lend further support to the role that methoxy and formate species play as intermediates in the catalytic mechanisms, but also provide a path forward for improving rates by means other than resorting to higher noble metal loadings.

Keywords Water gas shift · Low temperature water gas shift · Methanol steam reforming · WGS · LTS · Fuel processor · Platinum · Pt · Ceria · CeO_2 · Alkali · Dopants · Electronic effect · Sodium · Na

H. N. Evin · G. Jacobs · U. M. Graham · G. Thomas · B. H. Davis (✉)
Center for Applied Energy Research, 2540 Research Park Drive, Lexington, KY 40511, USA
e-mail: davis@caer.uky.edu

J. Ruiz-Martinez
Laboratorio de Materiales Avanzados, Departamento de Química Inorgánica, Universidad de Alicante, Apartado 99, 03080 Alicante, Spain

A. Dozier
Chemical and Materials Engineering Department, University of Kentucky Electron Microscopy Center, A004 ASTeCC Building 0286, Lexington, KY 40506, USA

1 Introduction

Alkali dopants are often used to promote water–gas shift [1–18] and methanol synthesis [4, 5] rates over metal/oxide heterogeneous catalysts. In 1981, based on an earlier report by Wagner and Somorjai [2] who indicated that NaOH coating improved liquid photolysis rates over $Pt/SrTiO_3$, Sato and White [3] added a NaOH coating to Pt/TiO_2, and found an improvement in the photocatalyzed water–gas shift rate. With 7 wt% NaOH added, the time to achieve complete CO conversion was cut in half.

Guidelines for the preparation of Cu and Zn bifunctional catalysts for reactions such as water gas shift, methanol synthesis, and higher alcohol synthesis, were presented by Klier [4, 5]. Although Klier focused primarily on methods to interdisperse copper with the oxide phase to guarantee a small Cu cluster size, the promoting influence of alkali dopants was also discussed, where the general trend over the

same series of reactions was found to be Cs > Rb > K > Na, Li. Klier suggested that the alkali should be present at concentrations less than a monolayer such that the hydrogen transfer reactions could take place without being impeded, while at the same time the basic function of the alkali could influence the concerted surface mechanism.

While Klier and coworkers [4, 5] observed a doubling of the water–gas shift rate on high surface area Cu/ZnO catalysts with the addition of Cs, Campbell et al. [6] observed a much greater promotion with Cs addition of 15 for Cu(111). Cs addition was suggested to assist in dissociating H_2O, their proposed rate limiting step. They indicated that dissociative adsorption of H_2O is important for either a formate or redox mechanism, and therefore, the explanation for Cs promotion can influence either mechanism. Later, Campbell and coworkers [7] offered a very different explanation for the promoting effect of Cs in studies over Cu(110). In kinetic studies using a low H_2O/CO ratio with 10 Torr H_2O and 26 Torr CO, they found that while previously the reaction rate was first order in H_2O and zero order in CO, on the optimally Cs-promoted surface, the reactant orders changed to zero order in H_2O and 0.5 order on CO, suggesting that dissociative adsorption of H_2O was no longer rate determining. They proposed a redox mechanism to describe the catalysis of both the clean and Cs doped surfaces, with Cs playing a role of O mediator among CO_2, H_2O, and CO, where Cs is primarily in the form of carbonate.

Basinska and Domka [8, 9] showed that addition of most alkali metals (Na, and especially K, Rb, or Cs) to Ru promoted α and δ-Fe_2O_3 led to remarkable improvements in the water–gas shift rates. Jozwiak and coworkers [10] explored the reducibility of Fe oxide, Ru/Fe oxide, and Na promoted Ru/Fe oxide catalysts by TPR (H_2 and CO) and additional methods, and the authors identified a link between the water–gas shift activity and the reduction of Fe_3O_4 to Fe_2O_3. The authors concluded that both Ru and Na facilitate the reduction step.

Luukkanen and coworkers [11, 12] reported enhanced activity over heterogenized polypyridine Ru complexes [$Ru(L)(CO)_2X_2$ on silica (e.g., $\sim$1.6% loading of Ru by weight), where the ligand L was either bipyridine or methyl substituted bipyridine and X=Cl, H, SCN, or $COOCH_3$] in the temperature range 100–160 °C when catalysts were activated using a new procedure that included the addition of either Na_2CO_3 or NaOH.

Brooks, et al. [13, 14] found through combinatorial screening methods a remarkable improvement in Pt/ZrO_2 catalysts for fuel processors for use in fuel cell applications by doping the catalysts with alkali. Over 250,000 experiments were carried out by synthesizing catalyst libraries on 4" wafers, and screening with a Symyx high throughput scanning mass spectrometer. Among the promising compositions discovered was an important improvement when Pt/ZrO_2 was doped with Na alone or in combination with V. Pigos et al. [15, 16] characterized the catalysts by DRIFTS spectroscopy measurements, and found that formate species were more reactive on the Na doped catalysts. Over Rh/ceria catalysts, Shido and Iwasawa [19] had previously demonstrated that the rate limiting step was C–H bond breaking of formate. Interestingly, Pigos et al. [15, 16] found that formate C–H stretching bands especially were strongly shifted to lower wavenumbers upon CO adsorption. In transient formate decomposition experiments both in the presence and absence of steam, Pigos, et al. [15–18] reported that formates over PtNa/ZrO_2 decomposed at twice the rate of those observed on Pt/ZrO_2 without Na. Furthermore, in steady state water–gas shift tests, the coverage of formate species was found to be more limited (i.e., by the water–gas shift rate) in DRIFTS for the Na promoted catalysts relative to those without Na. A more comprehensive analysis of Group I alkali promoters was carried also carried out [19], and while Li and K were found to promote the WGS rate, Na was found to provide the greatest benefit. The authors attributed the promoting effect of the alkali dopant to the enhanced reactivity of the formate C–H bond.

Recently, building directly on the earlier findings of Pigos et al. [15, 16], we determined that alkali dopants also electronically modify the ν(CH) vibrational mode of formate species over Pt/ceria catalysts [20], systematically shifting the band to lower wavenumber with (a) increasing alkali dopant level or (b) increasing alkali atomic number at equivalent atomic loadings. However, it was found that the type and loading of alkali also can negatively impact additional catalyst structural/chemical parameters, such as BET surface area, the Pt-ceria interfacial synergy, and the stability of carbonate species, which is also likely related to the Pt-ceria interface. In this follow-up investigation, the first aim was to explore the impact of low alkali doping levels using the lower atomic number Group 1 promoters during low temperature shift. Furthermore, since methanol steam reforming has been proposed to involve methoxy and formate species over Pt/ceria and Pt/thoria catalysts [21, 22], the second goal was to determine if these alkali promoters could influence the stability of both methoxy group and formate C–H bonds, since the dehydrogenation of these species is proposed to be important during the catalytic cycle based on kinetic isotope effect studies [21, 22].

2 Experimental

2.1 Catalyst Preparation

High surface area ceria was prepared via homogeneous precipitation of the nitrate in urea with aqueous ammonia in

a procedure similar to Li et al. [23], whereby urea decomposition is a slow process resulting in a more homogeneous precipitation. Appropriate amounts of $Ce(NO_3)_3 \cong 6H_2O$ (Alfa Aesar, 99.5%) and urea (Alfa Aesar, 99.5%) were dissolved in 600 mL of deionized water. The mixture was then heated at 90–100 °C with constant vigorous stirring. The precipitate was filtered, washed repeatedly with deionized water, and dried in an oven at 110 °C overnight. The dried precipitate was then crushed and calcined in a muffle furnace at 400 °C for 4 h. Pt was added by incipient wetness impregnation (IWI) of tetraammine platinum (II) nitrate (Alfa Aesar). The resulting catalyst was dried at 110 °C for 24 h, and then calcined at 300 °C for 3 h. The alkali was added by IWI following the calcination using a loading solution containing the corresponding alkali nitrate of Li, Na, K, Rb, or Cs. The catalyst was re-calcined at 300 °C for 3 h. The low alkali doping series was prepared with equivalent atomic loading based on 0.5%Na by weight.

2.2 X-ray Diffraction

Powder diffractograms on calcined catalysts were recorded using a PANalytical X'Pert diffractometer, Cu Kα ($\lambda = 0.154$ nm) as a radiation source. The conditions were as follows: scan rate of 0.02°/step, scan time of 1.53 s/step over a 2θ range of 5–90°.

2.3 BET Surface Area

BET surface area measurements were carried out using a Micromeritics Tristar 3000 gas adsorption analyzer. A weight of approximately 0.25 g of sample was used for each test. After being loaded into a Pyrex/Quartz glass cell, the samples were outgassed at 160 °C overnight. Nitrogen adsorption was carried out at its boiling temperature.

2.4 Temperature Programmed Reduction (TPR) and Thermogravimetric Analysis (TGA)

TPR was conducted using a Zeton-Altamira AMI-200 unit, which was equipped with a thermal conductivity detector (TCD). Argon was used as the reference gas, and 10%H_2 (balance Ar) was flowed at 30 cm^3/min as the temperature was increased from 50 °C to 800 °C at a ramp rate of 10 °C/min.

2.5 Temperature Programmed Desorption Mass Spectrometry (TPD-MS) of adsorbed CO_2

CO_2 is an important probe molecule for determining the basicity of metal/oxide catalysts [24]. The catalysts were treated *in-situ* in a Micromeritics AutoChem II 2920 chemisorption analyzer under the following conditions: the samples were first reduced at 300 °C for 8 h using 50 cm^3/min of 10% H_2 in Ar stream. After that, the samples were cooling down to 100 °C in a flowing 50%CO_2 in helium. After flushing with He, TPD was performed in He up to 700 °C, and the ramp rate was 10 °C/min. CO_2 desorbed was measured by a Pfeiffer/Balzers Thermostar mass spectrometer coupled to the Micromeritics system.

2.6 Diffuse Reflectance Infrared Fourier Transform Spectroscopy (DRIFTS)

A Nicolet Nexus 870 was used, equipped with a DTGS-TEC detector. A high pressure/high temperature chamber fitted with ZnSe windows was utilized as the WGS reactor for in-situ steady state and transient reaction measurements. The gas lines leading to and from the reactor were heat traced, insulated with ceramic fiber tape, and further covered with general purpose insulating wrap. Scans were taken at a resolution of 4 to give a data spacing of 1.928 cm^{-1}. Typically, 256 scans were taken to improve the signal to noise ratio. However, for transient experiments, 32 scans were required for the forward (steam-assisted) formate decomposition tests at 130 °C and 25 scans were used to decompose the methoxy species in steam at 160 °C. The sample amount was 40 mg.

A steam generator consisted of a downflow tube packed with quartz beads and quartz wool heated by a ceramic oven and equipped with an internal thermocouple. The lines after the steam addition were heat traced. The steam generator and lines were run at the same temperature as that of the in-situ sample holder of the DRIFTS cell. Water was pumped by a precision ISCO Model 500D syringe pump into a steam generator via a thin needle welded to a 1.6 mm line.

Feed gases (UHP) were controlled by using Brooks 5850 series E mass flow controllers. Iron carbonyl traps consisting of lead oxide on alumina (Calsicat) were placed on the CO gas line. All gas lines were filtered with Supelco O_2/moisture traps.

Catalysts were first reduced at 300 °C using H_2:N_2 (100 cm^3/min:130 cm^3/min). During CO adsorption (250 °C), the flows were maintained at 3.75 cm^3/min CO and 130 cm^3/min N_2. The catalyst was then cooled to 130 °C in flowing CO. During steam-assisted forward formate decomposition, the flow rates were 67.5 cm^3/min of N_2 and 62.5 cm^3/min of steam. Methanol adsorption was carried out by passing 67.5 cm^3/min of N_2 through a bubbler and saturating the surface of the reduced catalyst with methanol at 160 °C. The decomposition of methoxy species was carried out using 67.5 cm^3/min of N_2 and 62.5 cm^3/min of steam. Following steaming of formate (WGS) and

methoxy/formate (SRM) species, the catalyst was purged with N_2 to assess the surface carbonate species formed.

2.7 Testing in a Fixed Bed Reactor

Steady state CO conversion measurements were conducted in a fixed bed reactor consisting of a 0.5 in. stainless steel tube with an internal thermocouple. Experiments were conducted using 40 mg of catalyst diluted to 0.4 g with silicon carbide. The catalyst bed was supported on a bed of quartz glass wool. The description of the steam generator, gas delivery system, and ancillary equipment is provided in Section 2.6. Catalysts were activated in H_2 (100 cm^3/min at 300 °C) for 1 h prior to reaction testing. For low temperature shift, the conditions were chosen to simulate those of the low temperature shift reactor of a fuel processor, with the exception that CO_2 was not included in the tests. The gas flows were 3.75 cm^3/min CO, 62.5 cm^3/min H_2O, and 67.5 cm^3/min H_2. For methanol steam reforming, analogous conditions were selected as used in water–gas shift (3.75 cm^3/min CH_3OH, 62.5 cm^3/min H_2O, and 67.5 cm^3/min H_2) in order to maintain experimental control. That is, the moles of carbon-containing reactant were equivalent between the two cases, all other conditions being identical.

2.8 High Resolution Transmission Electron Microscopy

High resolution transmission electron microscopy (HR-TEM) characterization was carried out using a JEOL 2010F field emission electron microscope operated at an accelerating voltage of 200 kV. The instrument was equipped with an Emispec EsVision computer control system for digital beam control and Gatan digital Micrograph including a Gatan CCD multiscan camera. In addition the JEOL 2010F has a Fischione High Angle Annular Dark Field (HAADF) detector for scanning transmission electron microscopy (STEM) imaging with the ability to obtain a STEM probe of better than 2 Å and a point-to-point resolution of 0.5 nm. Prior to HR-TEM analysis all sample material was reduced ex-situ in flowing H_2 at 300 °C and subsequently passivated at room temperature. Catalyst powder was dispersed onto 200 mesh Cu grids with lacy carbon supports.

3 Results and Discussion

3.1 Preliminary Characterization

The ceria was examined by powder XRD to estimate the crystallite domain size. The ceria had a crystallite domain size of between 8.0 and 9.0 nm, as determined by line broadening analysis using the integral breadth method with Winfit software (Stefan Krumm, 1997). BET results for the calcined catalysts are provided in Table 1. The addition of alkali dopants led to a decrease in the BET surface area over the entire series, with the higher atomic number alkali metals generally resulting in lower surface areas. However, the results may be misleading, as they are indicative of the non-activated state of the catalyst, where a high concentration of surface carbonates was observed by infrared spectroscopy. A significant fraction of the carbonates was observed in infrared spectroscopy to decompose after the reduction step. The average pore radius was found to increase as a function of alkali dopant atomic number relative to the reference catalyst; this is likely attributed to blocking of the narrower pores by alkali compounds, and further supported by the decrease in pore volume observed.

Table 1 BET surface area and porosity results

Catalyst	BET SA (m^2/g)	Pore volume (cm^3/g)	Average pore radius (nm)
Reference catalysts			
Ceria	115.3	0.0850	1.47
2%Pt/ceria	109.4	0.0862	1.57
Low alkali doping (equivalent atomic content)			
2%Pt/0.15%Li/ceria	102.5	0.0817	1.59
2%Pt/0.5%Na/ceria	87.2	0.0670	1.53
2%Pt/0.9%K/ceria	73.7	0.0606	1.64
2%Pt/1.9%Rb/ceria	76.9	0.0684	1.77
2%Pt/2.9%Cs/ceria	66.4	0.0626	1.88

Results of H_2-TPR are depicted in Fig 1. The unpromoted ceria sample shows that reduction proceeds at two distinct temperatures. The low temperature peak, situated in the range of 450–500 °C, is typically ascribed to reduction of the ceria surface shell [25, 26] involving the removal of surface capping oxygen atoms, while the second peak, at much higher temperature (>700 °C) is assigned to reduction of bulk ceria. As observed in previous investigations [23, 27], addition of metal clusters (e.g., Pt) facilitates the surface reduction step to lower temperatures, while having little impact on the bulk reduction. It has been demonstrated that the reduction of the ceria surface shell is actually a more complicated process, and involves the formation of Type II bridging OH groups associated with the reduced Ce^{3+} defects, as well as the decomposition of carbonate species [27]. The former process can involve H_2 dissociation on the metal and spillover of H· to the cerium oxide surface and/or the dissociation of H_2O at the oxygen vacancies [27]. In the case of these lower alkali-doped samples (Fig. 1), there is an interesting splitting of the peak, while the overall peak area does not significantly change. The catalyst reduces over a wider

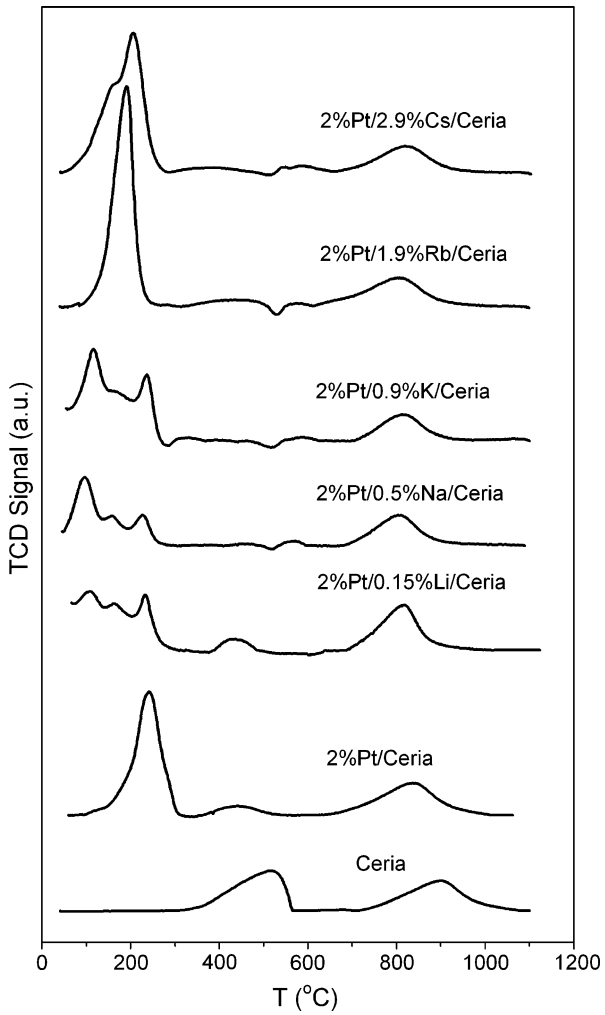

Fig. 1 TPR profiles of low alkali-doped Pt/ceria catalysts, relative to the reference catalyst samples

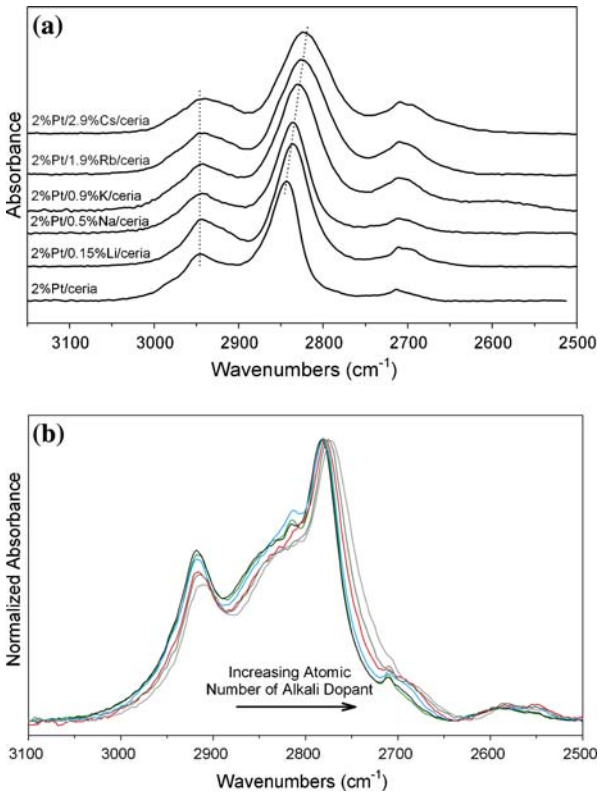

Fig. 2 (**a**) Formate and (**b**) methoxy ν(CH) band position as a function of alkali type for the low alkali doping series

range from 75 to 250 °C. This may be due to the presence of alkali in contact with a fraction of the metal particles, which may alter the interaction of the metal with the oxide.

3.2 Low Temperature Water–Gas Shift

The first DRIFTS experiment was to observe if the alkali exerted an impact on the ν(CH) band of the adsorbed formate molecule, as was observed in the case of Pt/ZrO_2 alkali (Li, Na, and K) doped samples [15–18]. Figure 2a in combination with Table 2 show that there is a systematic decrease in the band position corresponding to ν(CH) with increasing atomic number of the alkali metal. There are at least two additional bands within the vicinity of the main formate ν(CH) stretching band. For example, while Binet et al. [28] indicated that the band at ca. 2950 cm^{-1} corresponds to a coupling of the ν_s(OCO) mode with δ(CH) and that the lower wavenumber band at ca. 2710 cm^{-1} corresponds to 2δ(CH), others have assigned the higher wavenumber band to a ν(CH) band for bridge-bonded formate [29] and the lower wavenumber band to ν(CH) of formaldehyde [30]. In this contribution, we have adopted the assignments of Binet et al. [28], as shown in Table 2. There is clearly a decrease in the band positions for 2δ(CH) and ν_s(OCO) + δ(CH) as a function of the atomic number of the alkali metal present. There are a number of competing theories for how the alkali dopant may impact the strength of a bond. First, the effect may be geometric in nature, or electronic. Regarding the latter, one common viewpoint in the catalysis literature is that the alkali may interact with a molecule through an electrostatic force. Ponec [31] found that doping Pt/SiO_2 with K led to an improvement in the n-hexane turnover rate during aromatization, and proposed that the alkali could assist in closing the ring of the adsorbed intermediates through an electrostatic effect between the cation and the adsorbed intermediate. In turn, this would accelerate the ring closure turnover rate of the adsorbed intermediate (i.e., in that case, perhaps adsorbed hexatriene). Similarly, it is possible that an electrostatic interaction may induce a weakening of the formate C–H bond, leading to a decrease in the band position. Another

Table 2 Formate C–H and other relevant IR band positions upon CO adsorption at 225 °C using the assignments of Lavalley and coworkers [28]

Catalysts	Band position (cm^{-1})				
	ν(CH)	δ(CH) + ν_S(OCO)	2δ(CH)	ν(OCO)[a]	ν(CO) on Pt
Reference catalyst					
2%Pt/ceria	**2843**	**2945**	2713	**1578, 1298**	**2023**
				1607, 1470, 1386, 1325	2080–1856
Low alkali doping series					
2%Pt/0.15%Li/ceria	**2838**	**2943**	2711	**1585, 1293**	**2020**
				1476(sh), 1383, 1320(sh)	2085–1845
2%Pt/0.5%Na/ceria	**2836**	**2943**	2711	**1589, 1295**	**1998**
				1475(sh), 1394, 1379, 1200(sh)	2073–1830
2%Pt/0.9%K/ceria	**2830**	**2943**	2710	**1591, 1288**	**1965**
				1378	2062–1833
2%Pt/1.9%Rb/ceria	**2826**	**2941**	2710	**1596, 1301**	**1954**
				1373, 1340	2045–1813
2%Pt/2.9%Cs/ceria	**2824**	**2940**	2709	**1607, 1272**	**1951**
				1370, 1336, 1301	2047–1829

Major bands are highlighted in boldfaced type

[a] Formate and carbonate bands

common viewpoint is that the alkali can transfer charge [32]. This has also been suggested to occur during aromatization of n-hexane over Pt/KL catalysts, where charge transfer from K to the metal may enhance the electron density on Pt. In this case, charge transfer to the ceria component may have an indirect impact on the formate C–H bond. Finally, a third viewpoint is that the presence of the alkali may induce changes in the bonding of the formate to the catalyst surface, such that the formate may change from being bonded in a bidentate manner to another form (e.g., monodentate). This third viewpoint could be electronic or geometric in nature. Whatever the cause, since the rate limiting step of the low temperature water–gas shift reaction over metal/ceria catalysts has been proposed to be due to C–H bond breaking of formate intermediate, the shift of the position of the formate ν(CH) band as observed in DRIFTS is of considerable interest, as it suggests a weakening of the C–H bond.

Figure 3 (left) examines the forward decomposition of the formate species at 130 °C in the presence of H_2O over the Li and Na-doped catalysts in comparison with the 2%Pt/ceria reference catalyst. It is evident from the Fig. 3 (right) that, while formate is the main species detected upon CO adsorption over each catalyst sample, containing both formate ν(CH) and asymmetric (i.e., $\sim$1580 cm^{-1}) and symmetric ($\sim$1375 cm^{-1}) ν(OCO) modes [33], the main species following steaming are carbonates. This is clearly the case, as the bands for ν(CH) decrease to virtually nil while the band positions for ν(OCO) modes are slightly shifted in position, indicating the formation of a new species. The rate of the formate decomposition appears to be accelerated in the case of the alkali-doped catalysts, where the 1/4-life is considerably shortened (Table 3).

Table 4 shows that the Li and Na-doped catalysts exhibited higher water–gas shift activity than the 2%Pt/ceria reference catalyst. Table 3 suggests that there is a link between the relative water–gas shift rates as observed in fixed bed reactor tests and the relative formate decomposition rates over the series of catalysts tested. Figure 4 displays CO_2 TPD-MS results over the series of alkali-doped catalysts. A fraction of CO_2 was held-up over the higher atomic number alkali-doped samples, being released only at higher temperatures. However, CO_2 holdup was not found to be an issue for the lower atomic number alkali-doped catalysts (i.e., Li and Na).

3.3 Methanol Steam Reforming

DRIFTS was used to assess whether the alkali exerted an impact on the ν_a(CH) and ν_s(CH) bands characteristic of the adsorbed methanol molecule. Figure 2b in combination with Table 5 show that there is a systematic decrease in the band positions corresponding to both ν_a(CH) and ν_s(CH) modes with increasing atomic number of the alkali metal. The ν(OC) band position is an important tool to assess the oxidation state of ceria catalysts [28, 34]. In all cases after H_2 reduction, only one major band (albeit asymmetric in nature) was observed with a peak maximum in the range of 1062–1065 cm^{-1}, depending on the alkali dopant present. This low wavenumber band indicates that the ceria is in a reduced state and that bridging methoxy species are

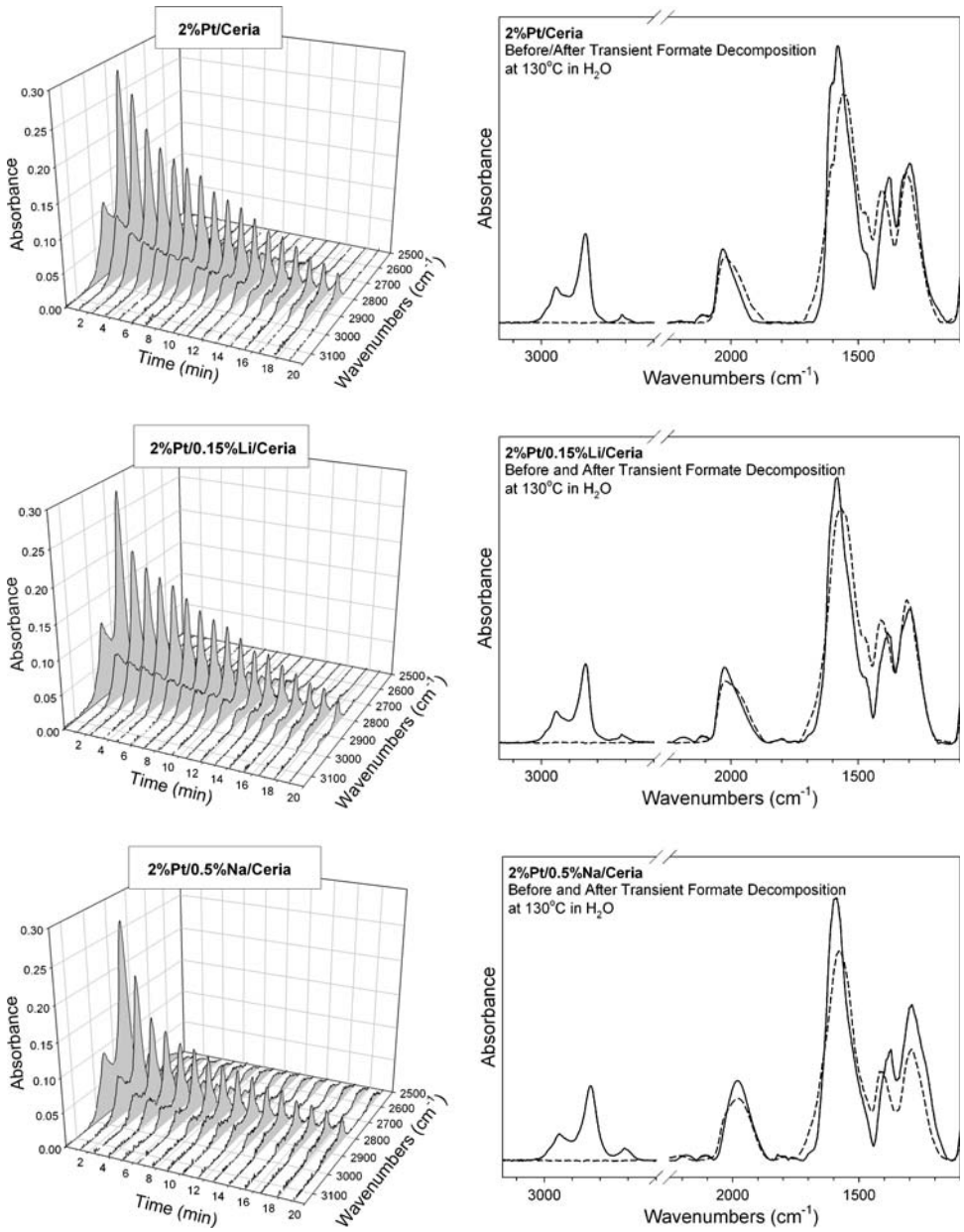

Fig. 3 (left) Transient formate decomposition in steam at 130 °C and (right) before and after decomposition snapshots for the Li and Na-doped catalysts relative to the undoped 2%Pt/ceria catalyst. Formate is converted to carbonate species

Table 3 Comparison of the relative formate decomposition rate with the relative water–gas shift rate

Catalyst	1/4-life (min)	K (min^{-1})	Relative sites from initial formate area	Relative formate decomp. rate	Relative X_{CO} at 275 °C
2%Pt/ceria	14.1	0.0983	1.00	1.00	1.00
2%Pt/0.15%Li/ceria	11.8	0.117	1.00	1.20	1.39
2%Pt/0.5%Na/ceria	11.1	0.125	1.11	1.41	1.49

present. It should be noted that for unreduced ceria, the main band present upon methanol adsorption is the Type I band, typically found in the range of 1105–1110 cm^{-1}.

During steaming of the methoxy species in the DRIFTS cell, it was found that the adsorbed methoxy species decomposed to formate species, in agreement with our earlier findings [21, 22]. The formate ν(CH), ν_s(OCO) + δ(CH), ν_a(OCO), and ν_s(OCO) bands are readily apparent during the decomposition of the methoxy groups (Fig. 5). The formates then further decompose to yield carbonate

Table 4 Conversion and selectivities during low temperature water–gas shift and methanol steam reforming

Catalyst	Water–gas Shift		Methanol steam reforming				
	T (°C)	% CO conv.	T (°C)	% MeOH conv.	% CO Select.	% CO_2 Select.	% CH_4 Select.
2%Pt/ceria	225	12.0	250	28.1	37.4	62.6	–
	250	23.0	300	65.2	31.1	68.9	–
	275	45.3	350	79.2	21.3	77.5	1.2
2%Pt/0.15%Li/ceria	225	14.0	250	28.7	50.8	49.2	–
	250	39.6	300	72.9	36.7	62.4	0.9
	275	63.3	350	85.1	15.8	83.4	0.8
2%Pt/0.5%Na/ceria	225	24.3	250	45.6	26.9	72.4	0.7
	250	51.0	300	87.3	17.3	81.9	0.8
	275	67.3	350	97.8	14.5	84.2	1.2

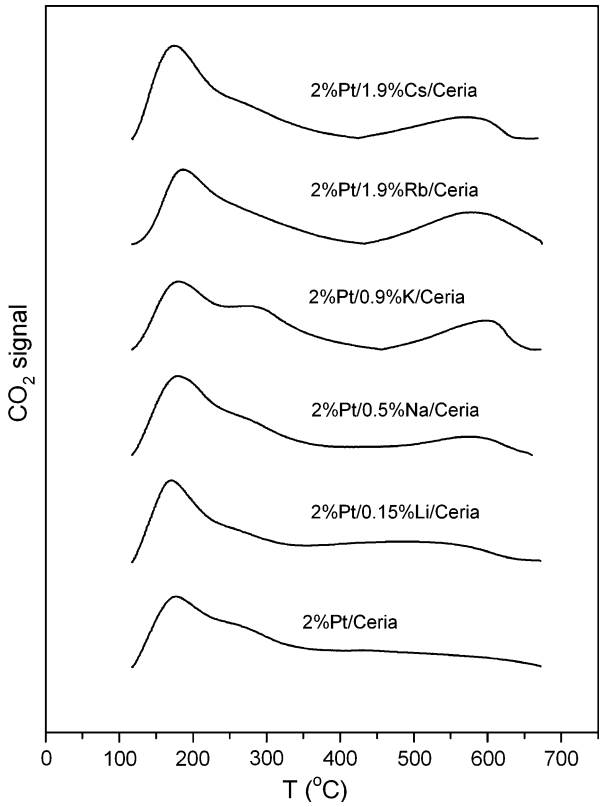

Fig. 4 Catalyst first reduced at 300 °C for 8 h. TPD-MS of adsorbed CO_2 with, moving upward, increasing alkali atomic number

species, as observed previously in the water–gas shift experiments. Purging the cell with N_2 after steaming easily reveals the presence of the newly formed carbonate species (Fig. 6). The important finding is that the alkali dopant exerts a positive influence on the rate of decomposition of the methoxy and formate bands during steaming at 160 °C. The hypothesis is that the alkali dopant weakens the C–H bonds of methoxy and formate species, facilitating their scission during the catalytic cycle. As shown in Table 4, the Li and Na dopants exert a positive impact on the methanol conversion rates. Moreover, the CO_2 selectivity in the case of the Na-doped catalyst was found to be higher than the Pt/ceria reference catalyst at all temperatures examined.

Table 5 Methoxy ν(CH) and ν(OC) IR band positions upon methanol adsorption at 160 °C using the assignments of Binet and coworkers [28, 34]

Catalysts	Band position (cm^{-1})		
	ν_a(CH)	ν_s(CH)	ν(OC)
Reference catalyst			
2%Pt/ceria	**2917**	**2781**	**1063**
Low alkali doping series			
2%Pt/0.15%Li/ceria	**2917**	**2779**	**1063**
2%Pt/0.5%Na/ceria	**2916**	**2778**	**1062**
2%Pt/0.9%K/ceria	**2916**	**2778**	**1062**
2%Pt/1.9%Rb/ceria	**2914**	**2775**	**1064**
2%Pt/2.9%Cs/ceria	**2911**	**2773**	**1065**

3.4 A Nano-structured Catalyst

The HR-TEM image provided in Fig. 7 with a 2 nm scale show ceria particles with a diameter between 2 and 5 nm. Very small Pt crystallites were clearly visible mainly in the 0.5–1.5 nm diameter range.

4 Conclusions

Doping Pt/ceria catalysts with the Group 1 alkali metals was found to lead to an important shift to lower wavenumbers of the γ(CH) modes of formate and methoxy species, suggesting weakening of the bonds. Li and Na-doped Pt/ceria

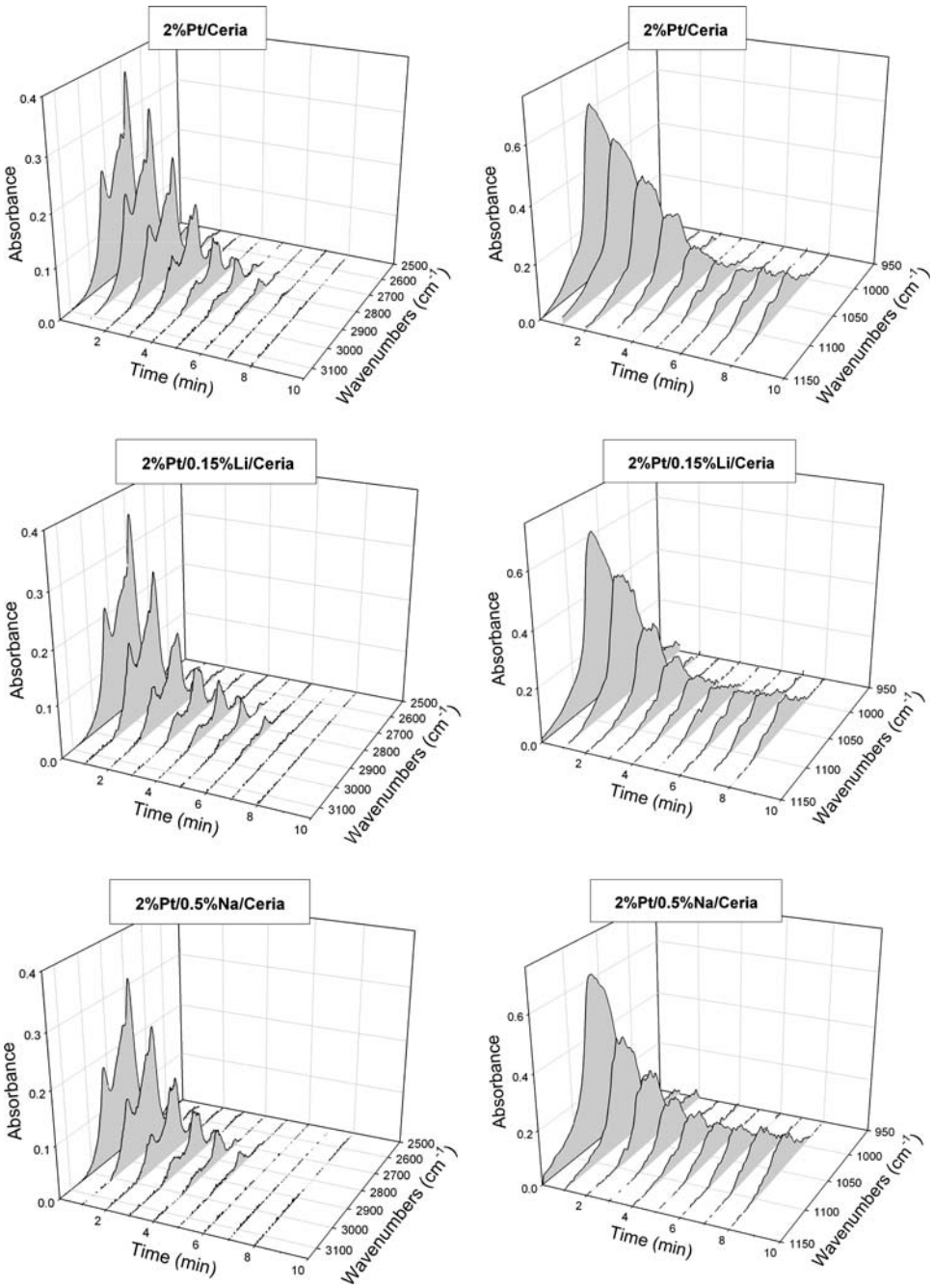

Fig. 5 (Left) *v*(CH) region and (right) methoxy *v*(CO) region during transient decomposition of methoxy species to formate, followed by decomposition of formate in steam (160 °C) for the Li and Na-doped catalysts relative to 2%Pt/ceria

catalysts displayed higher catalytic activity during low temperature water–gas shift and methanol steam reforming. Formate species, produced from the reaction of CO with Type II bridging OH groups, and methoxy species, generated from methanol adsorption, were reacted with steam at 130 °C and 160 °C, respectively, and both species were found to be more reactive relative to the undoped 2%Pt/ceria catalyst. While formate converted to carbonate species at 130 °C, steaming of methoxy species converted to formate species, prior to their decomposition to carbonate species. The results suggest that the alkali dopants weaken the C–H bonds, making them more reactive for dehydrogenation steps involved in the catalytic cycles. Increasing the atomic number of the alkali dopant over the Group 1 series resulted in increasing stability of a fraction of the carbonate. This was observed during TPD-MS measurements of the adsorbed CO_2 probe molecule by a systematic increase of a high temperature peak for a fraction of the CO_2 desorbed. The results not only lend further support to the role that methoxy and formate species play as intermediates

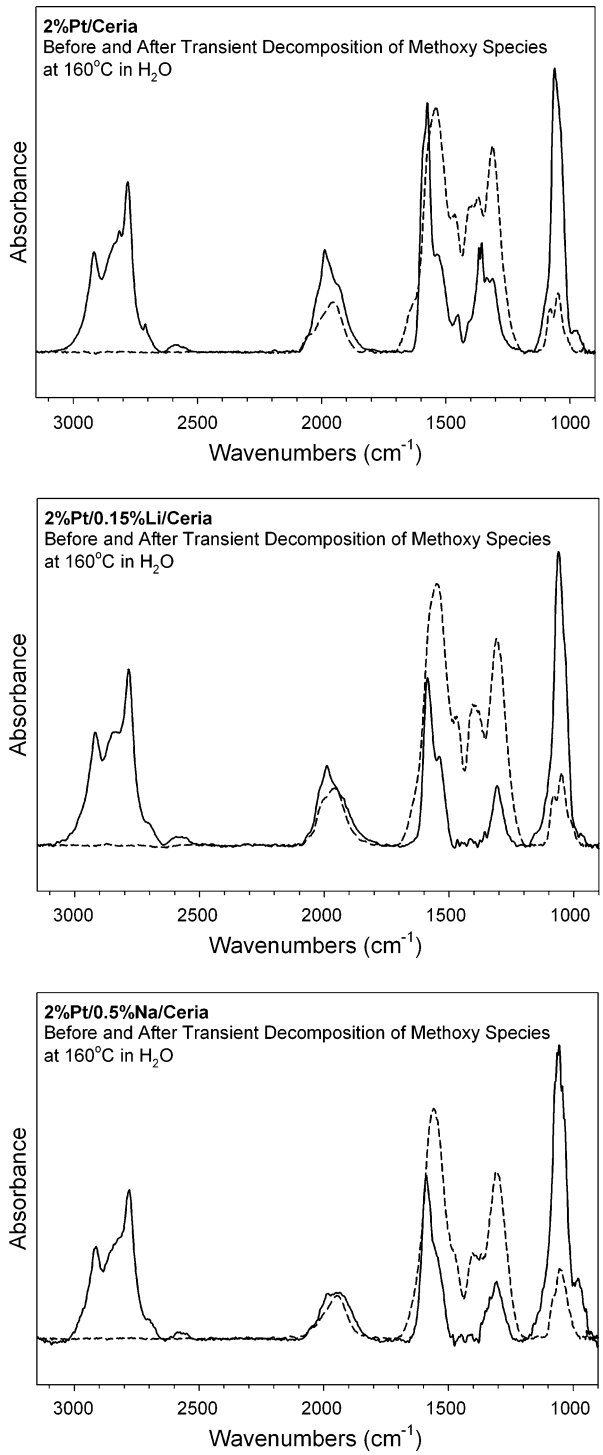

Fig. 6 Before and after snapshots of the transient decomposition of methoxy species in steam at 160 °C for the heavily alkali doped catalysts with equivalent atomic loading of alkali. Methoxy species are converted to formate, followed by conversion to carbonate species

in these catalytic mechanisms, but also provide a path forward for improving rates by means other than resorting to higher metal loadings.

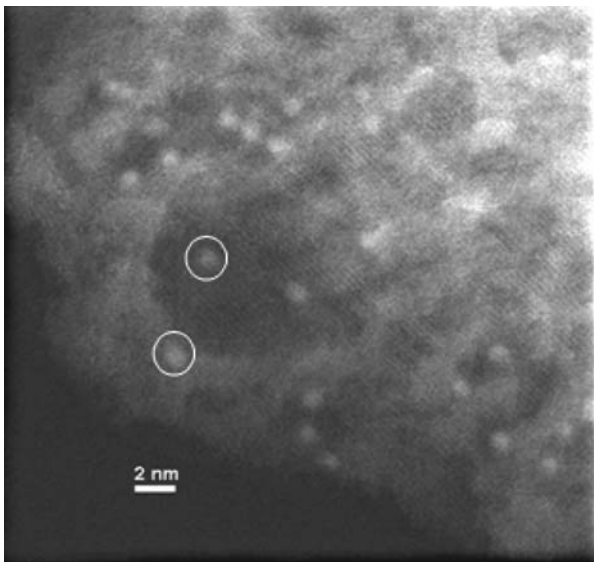

Fig. 7 HR-TEM image of 2%Pt/0.9%K/Ceria

Acknowledgments The work was sponsored by the Commonwealth of Kentucky.

References

1. Sato S, White JM (1980) J Am Chem Soc 102:7206
2. Wagner FT, Somorjai GA (1980) J Am Chem Soc 102:5494
3. Sato S, White JM (1981) J Catal 69:128
4. Vedage GA, Pitchai R, Herman RG, Klier K (1984) Proceedings of the 8th International Congress on Catalysis, Berlin, Germany, pp 47
5. Klier K (1992) Catal Today 15:361
6. Campbell CT, Koel BE, Daube KA (1987) J Vac Sci Technol A 5:810
7. Campbell JM, Nakamura J, Campbell CT (1992) J Catal 136:24
8. Basinska A, Domka F (1993) Catal Lett 17:327
9. Basinska A, Domka F (1997) Catal Lett 43:59
10. Jozwiak WK, Basinska A, Goralski J, Maniecki TP, Kincle D, Domka F (2000) Stud Surf Sci Catal 130: 3819
11. Luukkanen S, Homanen P, Haukka M, Pakkanen TA, Deronzier A, Chardon-Noblat S, Zsoldos D, Ziessel R (1999) Appl Catal 185:157
12. Luukkanen S, Haukka M, Kallinen M, Pakkanen TA (2000) Catal Lett 70:123
13. Brooks CJ, Hagemeyer A, Yaccato K, Carhart R, Herrmann M (2005) 19th North American Meeting of the Catalysis Society, May 22–27, Philadelphia
14. Yaccato K, Carhart R, Hagemeyer AG, Herrmann M, Lesik A, Strasser P, Turner H, Volpe1 AF, Weinberg H, Brooks CJ (2006) AIChE Spring National Meeting, April 23–27, Orlando
15. Pigos JM, Brooks CJ, Jacobs G, Davis BH (2006) DRIFTS Studies of platinum-based zirconia catalyst promoted with sodium discovered by combinatorial methods. Prepr Am Chem Soc Div Pet Chem
16. Pigos JM, Brooks CJ, Jacobs G, Davis BH (2006) Evidence of enhanced LTS water–gas shift rate with Sodium promoted Pt–ZrO_2-based catalyst discovered by combinatorial methods, AIChE Annual Meeting abstract

17. Pigos JM, Brooks CJ, Jacobs G, Davis BH (2007) Appl Catal A Gen 319:47
18. Pigos JM, Brooks CJ, Jacobs G, Davis BH (2007) Appl Catal A Gen 328:14
19. Shido T, Iwasawa Y (1993) J Catal 141:71
20. Jacobs G, Davis BH, Pigos JM, Brooks CJ (2007) Low temperature water–gas shift: weakening of formate C–H bond observed with alkali doping with Pt/ZrO_2 and Pt/CeO_2 catalysts, 20th North American Meeting of The Catalysis Society, June 17–22, Houston, TX
21. Jacobs G, Davis BH (2005) Appl Catal A Gen 285:43
22. Jacobs G, Patterson PM, Graham UM, Crawford AC, Dozier A, Davis BH (2005) J Catal 235:79
23. Li Y, Fu Q, Flytzani-Stephanopoulos M (2000) Appl Catal B 27:179
24. Lavalley JC (1996) Catal Today 27:377
25. Yao HC, Yu Yao YF (1984) J Catal 86:254
26. Laachir A, Perrichon V, Badri A, Lamotte J, Catherine E, Lavalley JC, El Fallah J, Hilaire L, Le Normand F, Quemere E, Sauvion GN, Touret O (1991) J Chem Soc Faraday Trans 87:1601
27. Jacobs G, Graham UM, Chenu E, Patterson PM, Dozier A, Davis BH (2005) J Catal 229:499
28. Binet C, Daturi M, Lavalley JC (1999) Catal Today 50:207
29. Shido T, Iwasawa Y (1992) J Catal 136:493
30. Li C, Sakata Y, Arai T, Domen K, Maruya KI, Onishi T (1989) J Chem Soc, Faraday Trans I 85:145
31. Fukunaga T, Ponec V (1997) Appl Catal A Gen 154:207
32. Larsen G, Haller GL (1989) Catal Lett 3:103
33. Holmgren A, Anderson B, Duprez D (1999) Appl Catal B 22:215
34. Binet C, Daturi M (2001) Catal Today 70:155